Phase Equilibria Study of the Binary Systems (1-Butyl-3-methylimidazolium Thiocyanate Ionic Liquid + Organic Solvent or Water)[‡]

Urszula Domańska,* M. Laskowska, and Aneta Pobudkowska

Physical Chemistry Division, Faculty of Chemistry, Warsaw University of Technology, Noakowskiego 3, 00-664 Warsaw, Poland

Received: February 3, 2009; Revised Manuscript Received: March 20, 2009

(Solid + liquid) phase equilibria (SLE) for the binary systems, ionic liquid (IL) 1-butyl-3-methylimidazolium thiocyanate [BMIM][SCN] with an alcohol (1-octanol, 1-nonanol, 1-decanol, 1-undecanol, or 1-dodecanol) or water, and (liquid + liquid) phase equilibria (LLE) for the binary systems of [BMIM][SCN] with an alkane (*n*-hexane, *n*-heptane, *n*-octane, *n*-nonane, or *n*-decane), benzene, an alkylbenzenes (toluene or ethylbenzene), tetrahydrofuran (THF), cycloalkanes (cyclohexane or cycloheptane), or ethers (di-*n*-propyl ether, di-*n*-butyl ether, di-*n*-pentyl ether, *n*-butylmethyl ether, *tert*-butylmethyl ether (MTBE), or *tert*-butylethyl ether (ETBE)) have been determined at ambient pressure. A dynamic method was used over a broad range of mole fractions and temperatures from 250 to 430 K. In the case of systems IL + alkane, cycloalkane, or ether, the mutual immiscibility with an upper critical solution temperature (UCST) was detected, and in the systems of IL + benzene, alkylbenzene, or THF, the mutual immiscibility with a lower critical solution temperature (LCST) was observed. UV−vis spectroscopy was used to determine the very small compositions of the IL in the *n*-hexane (about 2×10^{-5} IL mole fraction), benzene (about 2×10^{-3} IL mole fraction), cyclohexane (about 2×10^{-5} IL mole fraction), and THF (about 1.2×10^{-2} IL mole fraction). For the binary systems containing alcohol, it was noticed that with increasing chain length of an alcohol, the solubility decreases. The basic thermal properties of the pure IL, that is, the glass-transition temperature as well as the heat capacity at the glass-transition temperature, have been measured using a differential scanning microcalorimetry technique (DSC). Decomposition of the IL was detected by the simultaneous TG/DTA experiments. Well-known UNIQUAC, Wilson, and NRTL equations have been used to correlate the experimental SLE data sets for alcohols and water. For the systems containing immiscibility gaps {IL + alkane, benzene, alkylbenzene, cycloalkane, tetrahydrofuran, or ether}, the parameters of the LLE correlation have been derived using the NRTL equation.

Introduction

Ionic liquids (ILs) are a novel class of chemical compounds with interesting properties with potential applications in separation methods.[1–5] Their specific properties, that is, high selectivity in the separation of aliphatic hydrocarbons from aromatic hydrocarbons or thiophene from alkanes, make ILs interesting for new technologies.[6–9] Knowledge of the phase equilibria (solid + liquid equilibria, SLE, and liquid + liquid equilibria, LLE) is fundamental for the ILs to be effectively used as solvents in liquid−liquid extraction.[10–14]

Until recently, the most important and popular ILs considered as extractive solvents, imidazolium, tetraalkylammonium- and phosphonium-based ionic liquids with cation structures by alkyl, hydroxyl, alkoxyalkyl, or aromatic substituents, and bis-{(trifluoromethyl)sulfonyl}imide [NTf₂]⁻, alkylsulfate [RSO₄]⁻, trifluoroacetate [CF₃COO]⁻, and thiocyanate [SCN]⁻ anions, have attracted our attention. Usually, SLE and LLE of binary or ternary systems containing the IL and an alcohol, water, ether, ketone, or hydrocarbon have been measured by us.[1,5,8–14] This paper is a continuation of our wide-ranging investigation into ILs containing the thiocyanate anion.[9,15] Two thiocyanate-based ILs were investigated by us as a separation media for aromatic

and aliphatic hydrocarbons or thiophene and alkanes with very high selectivities and capacities.[9,15] The determination of activity coefficients at infinite dilution of organic solutes in the ionic liquid 1-ethyl-3-methylimidazolium thiocyanate [EMIM][SCN][9] and [BMIM][SCN][15] by gas−liquid chromatography (GLC) has been reported. The highest selectivity values ever published indicated that these two ionic liquids are the best for solvent extraction processes in different separating processes.

The purpose of this work is to present solubilities of 1-butyl-3-methylimidazolium thiocyanate [BMIM][SCN] ionic liquid in alcohols, water, alkanes, benzene, alkylbenzenes, cycloalkanes, THF, and ethers and compare them to the existing data of ILs with the same cation and different anions, that is, hexafluorophosphate, [PF₆]⁻, methylsulfate, [CH₃SO₄]⁻, and octylsulfate, [OcSO₄]⁻. We believe that this important information allows us make predictions of the phase behavior of unmeasured systems, at least in a semiquantitative way.

The characteristics investigated here include the effect of the alkyl chain length of the alcohols, alkanes, and ethers, the effect of the alkyl chain length on the benzene ring, and the type of anion with the same cation.
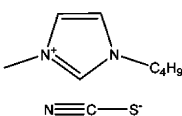
Experimental Procedures and Results

Materials. The studied ionic liquid, that is, 1-butyl-3-methylimidazolium thiocyanate [BMIM][SCN], was delivered by Fluka, Germany and was reported to have a mass fraction

* To whom correspondence should be addressed. E-mail: ula@ch.pw.edu.pl.

TABLE 1: Investigated Ionic Liquid Properties[a]

structure	name		
	1-butyl-3-methylimidazolium thiocyanate		
	abbreviation [BMIM][SCN]	M/g·mol^{-1} 197.3	$V_{m,1}^{298.15}$/cm^3·mol^{-1} 184.43
	CAS 344790-87-0	$\eta^{298.15}$/mPa·s 51.7± 0.1	$T_{g,1}$/K 181.6± 0.1
			$\Delta C_{p(g),1}$/JK^{-1}mol^{-1} 97.7 ± 3

[a] Given are the chemical structure, names, abbreviations, molar mass (M), CAS number, and measured thermophysical properties, including the molar volume ($V_{m,1}$) at 298.15 K, dynamic viscosity (η) at 298.15 K, glass-transition temperature ($T_{g,1}$), and heat capacity change at $T_{g,1}$ ($\Delta C_{p(g),1}$).

TABLE 2: Physicochemical Characteristics of Solvents (Literature Data) Utilized in the Correlation of the Experimental (Solid + Liquid) Phase Equilibrium Data[a]

	$(T_{fus,2})$/(K)	$(\Delta_{fus}H_2)$/(kJ·mol^{-1})	$(V_{m,2})$/(cm^3·mol^{-1})
1-octanol	258.35[b]	23.70[b]	158.50[b]
1-nonanol	268.15[c]	24.54[c]	174.95[c]
1-decanol	280.15[b]	28.79[b]	191.60[b]
1-undecanol	284.15[b]	33.61[b]	208.10[b]
1-dodecanol	296.95[b]	38.42[b]	224.70[b]
water	273.15	6.01	18.06[d]

[a] Given are the temperatures and enthalpies of fusion ($T_{fus,2}$ and $\Delta_{fus}H_2$, respectively) and the molar volumes ($V_{m,2}$) at 298.15 K. [b] Reference 16. [c] Reference 17. [d] Calculated from the density cited in ref 18.

purity > 0.95. The ionic liquid was purified by subjecting the liquid to a very low pressure of about 5×10^{-3} Pa at a temperature of about 300 K for approximately 5 h. The physicochemical properties of the IL are presented in Table 1. All utilized solvents were obtained from Sigma-Aldrich Chemie GmbH, Steinheim, Germany. Before use, they were fractionally distilled over different drying reagents to the mass fraction purity of ≥0.998. They were each stored over freshly activated molecular sieves of type 4 Å (Union Carbide) and checked by gas−liquid chromatography (GLC). Basic volumetric and thermophysical properties of the alcohols and water are tabulated in Table 2.

Water Content. The water content was analyzed by Karl Fischer titration (method TitroLine KF). Samples of [BMIM]-[SCN] and the solvents were dissolved in dry methanol and titrated with steps of 2.5 µL. The analysis showed that the water mass fractions in the solvents and in the mixtures with the ionic liquid were $<230 \times 10^{-6}$.

Differential Scanning Microcalorimetry (DSC). Basic thermal characteristics of the ionic liquid, that is, the glass-transition temperature ($T_{g,1}$) and the change of heat capacity at the glass-transition temperature, $T_{g,1}$ ($\Delta C_{p(g),1}$) have been measured using a differential scanning microcalorimetry technique (DSC) at the 5 K·s^{-1} scan rate with the power sensitivity of 16 mJ·s^{-1} and with the recorder sensitivity of 5 mV. The instrument (Perkin−Elmer Pyris 1) was time calibrated with the 99.9999 mol % purity indium sample. The calorimetric accuracy was ±3%, and the calorimetric precision was ±0.5%. The thermophysical properties are shown in Table 1, and the DSC diagram is shown as GRS 1 in the Supporting Information (SI). The average value of the glass-transition temperature was $T_{g,1}$ was (181.6 ± 0.1) K with a $\Delta C_{p(g),1}$ of (97.7 ± 3) J·mol^{-1}·K^{-1} (average over four scans).

Decomposition of Compounds. Simultaneous TG/DTA experiments were performed using a MOM Derivatograph - PC (Hungary). In general, runs were carried out using matched labyrinth platinic crucibles with Al_2O_3 in the reference pan. The crucible design hampered the migration of volatile decomposi-

tion products, reducing the rate of gas evolution and, in turn, increasing the contact time of the reactants. All TG/DTA curves were obtained at a 5 K·min^{-1} heating rate with a nitrogen dynamic atmosphere (flow rate of 20 dm^3·h^{-1}). The temperatures of decomposition are presented in GRS 2 in the SI. We can see that up to 523 K, the decomposition is not observed.

Phase Equilibria Apparatus and Measurements. A dynamic (synthetic) method for the solubility measurements was used in the present work. Details of the procedures have been described previously.[19] The ionic liquid was kept under nitrogen in a drybox during the short time of adding the solvent to the vessel. Mixtures {[BMIM][SCN] + solvent} were prepared by weighing the pure components with an uncertainty of 1×10^{-4} g. Mixtures were prepared by mass, and errors did not exceed 5×10^{-4} in mole fraction. The sample was heated very slowly (<2 K·h^{-1}) with continuous stirring inside of a Pyrex glass cell placed in a thermostat. The crystal disappearance temperatures, detected visually, were measured with an electronic thermometer P 550 (DOSTMANN electronic GmbH) with the probe totally immersed in the thermostatting liquid. The uncertainties of the temperature measurements were judged to be 0.05 K. The repeatability of the SLE/LLE experimental points was ±0.05 K. The results of the solubility measurements are presented in Tables 1S−5S (SI). The tables include direct experimental results of the SLE equilibrium temperatures, T^{SLE}, or of the LLE equilibrium temperatures, T^{LLE}, versus the ionic liquid mole fraction, x_1 for the system [BMIM][SCN] (1) + solvent (2). The visual method was not applicable at the very low mole fraction of the IL ($x_1 = 1 \times 10^{-5}$) mainly because of uncertainties and verticality of the saturated equilibrium curve.

UV−Vis Spectroscopy. UV−vis spectroscopy was only applied to determine the mole fraction of [BMIM][SCN] in the n-hexane-, benzene-, and cyclohexane-rich phases that coexists with an ionic-liquid-rich phase. For such an analysis, about 20 mL of a biphasic mixture (containing the mole fraction of about 0.01% of the IL) was thermostatted in the temperature-controlled thermostat (Lauda A 3, Germany) through the jacket of the vessel with stirring for about 8 h. After equilibration (18 h) and phase separation, a sample was taken out with a syringe from the solvent-rich phase (i.e., n-hexane) and was mixed with a known amount of 2-propanol (complete miscibility). The masses of both the sample and the diluent were determined by a balance (Mettler Toledo AE 240). A quartz cuvette (path length of 10 mm) was filled with the diluted 2-propanol solution of the IL, and the UV spectrum was recorded between 180 and 350 nm with a UV/vis spectrophotometer (Perkin−Elmer Life and Analytical Sciences, Shelton, U.S.A.). The reference cuvette was filled with the 2-propanol. The overall experimental uncertainty for the temperature was estimated to be 0.1 K. The photometric accuracy (NIST 930D Filter 1A) obtainable with
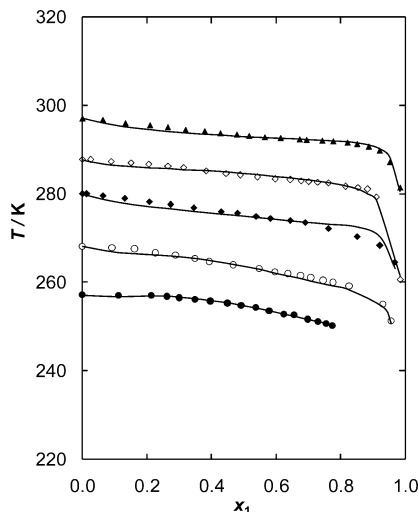
Phase Equilibria Study of the Binary Systems

J. Phys. Chem. B, Vol. 113, No. 18, 2009 **6399**

Figure 1. Experimental and calculated (solid + liquid) phase equilibria of {[BMIM][SCN] (1) + 1-alcohol (2)} binary systems; (●) 1-octanol; (○) 1-nonanol; (◆) 1-decanol; (◇) 1-undecanol; (▲) 1-dodecanol. Solid lines (—) have been calculated using the NRTL equation (for 1-octanol, 1-nonanol, 1-decanol, and 1-undecanol) and the Wilson equation (for 1-dodecanol).

the UV–vis spectrophotometer was ±0.001 A, and the repeatability was ≤0.001 A. The uncertainty in the mole fraction was 1×10^{-6}.

For the calibration process, several stock solutions including small quantities of ionic liquid dissolved in a large amount of solvent were prepared. Many series of UV spectra were recorded at $T = 293.15$ K, and for each sample, the obtained peaks were analyzed. For the pure IL and 2-propanol (background), the region of the interesting spectrum $A = f(\lambda)$ (minimum after the maximum) was 200–300 nm. For the solutions of the IL in solvent, that is, benzene, the region of the interesting spectrum was observed to be very narrow (220–244 nm). In this sensitive region, the absorbance (A) was a linear function of the mole fraction of the IL. The wavelength with the lowest correlation coefficient R^2 of a straight line was chosen. A more careful examination reveals that the interesting region of the spectrum measured here decreases with an increasing temperature. An analysis of the diagram's $T = f(x_1)$ indicates a subtle but clear wavelength, chosen for the binary system IL + solvent.

The UV–vis spectra for four binary systems are shown in GRS 3–6 in the SI for the hexane, benzene, cyclohexane, and THF, respectively.

Results

The data (temperature versus mole fraction of the IL) for the binary systems with alcohols, water, aliphatic hydrocarbons, aromatic hydrocarbons, cycloalkanes, and ethers are presented in Figures 1–6. The experimental (solid + liquid) phase equilibrium data for the systems [BMIM][SCN] + an alcohol or water is given in Table 1S in the SI and in Figures 1 and 2. The strong interaction between the IL and alcohols and the complete miscibility in the liquid phase was observed from methanol to 1-dodecanol at room temperature. It was possible to measure only the liquidus curves of alcohols or water in the ionic liquid at low temperatures. These mixtures reveal the simple eutectic systems with the eutectic points shifted to the rich ionic liquid mole fraction. On the basis of the investigated phase diagrams for the systems {[BMIM][SCN] + an alcohol or water}, the following trends can be noticed; the solubility of an alcohol in the IL decreases as the length of carbon chain of
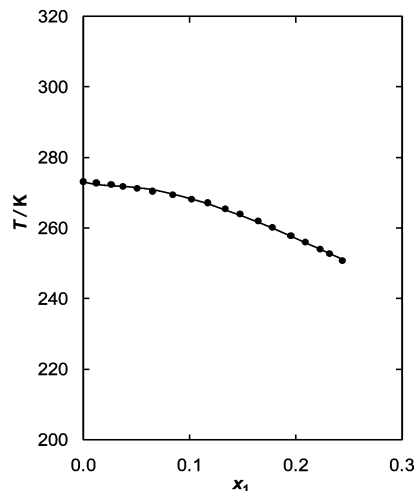

Figure 2. Experimental and calculated (solid + liquid) phase equilibria of the {[BMIM][SCN] (1) + water (2)} binary system. Solid lines (—) have been calculated using the UNIQUAC equation.
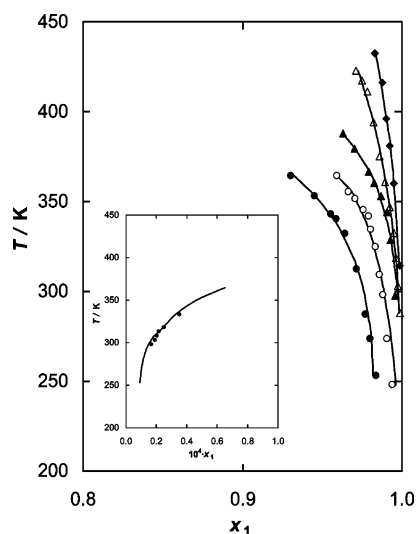

Figure 3. Experimental and calculated (liquid + liquid) phase equilibria of {[BMIM][SCN] (1) + aliphatic hydrocarbon (2)} binary systems; (●) *n*-hexane; (○) *n*-heptane; (▲) *n*-octane; (△) *n*-nonane; (◆) *n*-decane. Solid lines (—) have been calculated using the NRTL equation.

an alcohol increases. It was observed that the solubilities of the [BMIM][SCN] in alcohols and water were lower than the ideal solubility (see activity coefficients, $\gamma_1 > 1$ in Table 1S in the SI). In the case of each alcohol, solubilities of the [BMIM][SCN] in comparison with those of the ionic liquids with the same cation and different anion are similar. For example, 1-butyl-3-methylimidazolium methylsulfate, [BMIM][CH₃SO₄], and 1-butyl-3-methylimidazolium octylsulfate, [BMIM][OcSO₄], reveal complete miscibility with alcohols in the liquid phase from ethanol to 1-undecanol.[20,21] This is unquestionably the influence of the anion of the IL on its phase behavior with the same solvent. The solubility of water in [BMIM][SCN] is lower than that in 1-octanol and 1-nonanol and higher than that in other alcohols measured in this work. This is a simple dependence on the melting temperature of the solvent.

The experimental results for systems {[BMIM][SCN] + aliphatic hydrocarbon} are given in Table 2S in the SI and in Figure 3. The (liquid + liquid) phase equilibria, LLE, were observed for these systems as usual. The solubility of *n*-alkane in the [BMIM][SCN] decreases with an increase of the alkyl
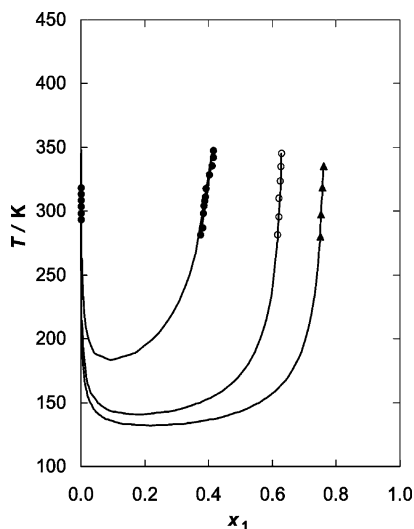
Figure 4. Experimental and calculated (liquid + liquid) phase equilibria of {[BMIM][SCN] (1) + benzene or *n*-alkylbenzene} (2) binary systems; (●) benzene; (○) toluene; (▲) ethylbenzene. Solid lines (—) have been calculated using the NRTL equation.
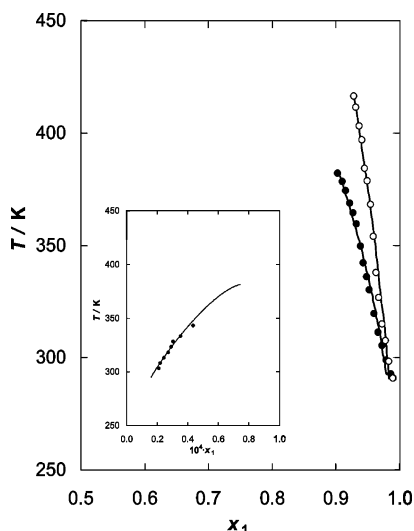
Figure 5. Experimental and calculated (liquid + liquid) phase equilibria of {[BMIM][SCN] (1) + cycloalkane (2)} binary systems; (●) cyclohexane; (○) cycloheptane. Solid lines (—) have been calculated using the NRTL equation.
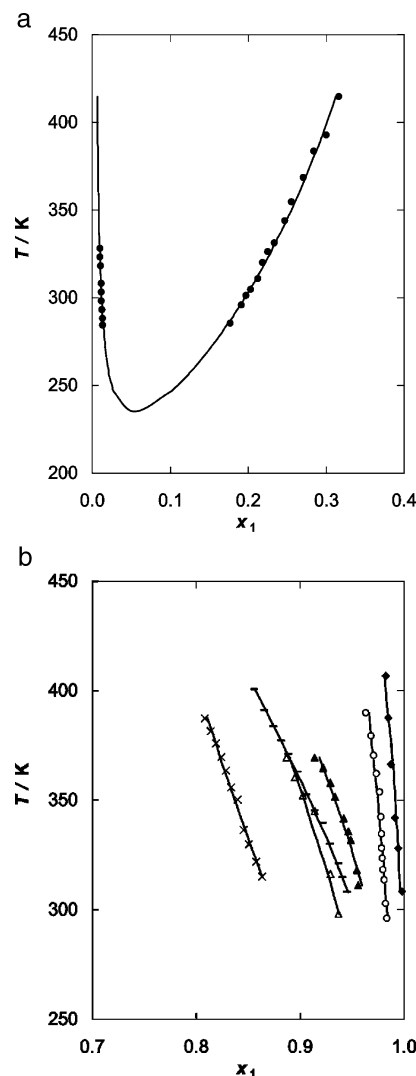
Figure 6. (a) Experimental and calculated (liquid + liquid) phase equilibria of {[BMIM][SCN] (1) + tetrahydrofuran (2)} binary system; (●) experimental points. Solid lines (—) have been calculated using the NRTL equation. (b) Experimental and calculated (liquid + liquid) phase equilibria of {[BMIM][SCN] (1) + ether (2)} binary systems; (▲) di-*n*-propyl ether; (○) di-*n*-butyl ether; (◆) di-*n*-pentyl ether; (△) *n*-butylmethyl ether; (×) *tert*-butylmethyl ether; (-) *tert*-butylethyl ether. Solid lines (—) have been calculated using the NRTL equation.

chain length of *n*-alkane from C_6 to C_{10} (see Figure 3); for the longer chain of *n*-alkane, the upper critical solution temperature (UCST) is shifted to the higher temperatures and to the higher IL mole fraction. These experimental results were compared to the previously measured binary systems with [BMIM][CH$_3$SO$_4$], [BMIM][OcSO$_4$], 1-butyl-3-methylimidazolium hexafluorophosphate [BMIM][PF$_6$], and 1-butyl-3-methylimidazolium 2-(2-methoxyethoxy)ethylsulfate [BMIM][MDEGSO$_4$].[20–24] The comparison of the solubility of *n*-hexane in the ILs with the same cation is presented in Figure 7. The solubility of *n*-hexane in the IL increases in the order [BMIM][OcSO$_4$] > [BMIM][CH$_3$SO$_4$] > [BMIM][PF$_6$] > [BMIM][MDEGSO$_4$] > [BMIM][SCN]. Replacing the anion [OcSO$_4$]$^-$ on [SCN]$^-$ decreases the solubility more than 100%. New data presented here show the very low solubility of *n*-alkanes in the [BMIM][SCN] and nearly complete immiscibility in the liquid phase with the IL. It was also confirmed by the values of the activity coefficients at infinite dilution for *n*-alkanes in [BMIM][SCN].[15] The very high values of the activity coefficients at infinite dilution for *n*-alkanes in

[BMIM][SCN] were observed in comparison with different ILs with the same cation.[15] In the systems of {[BMIM][SCN] (1) + *n*-alkane (2)}, the consolute temperatures were at a very low mole fraction of the IL and were undetectable with the visual method. UV−vis spectroscopy was applied in the present work to determine the mole fraction of the IL in the solvent-rich phase of *n*-hexane. A spectroscopic method was used also to detect the solubility of benzene, cyclohexane, and THF in the solvent-rich phase.

Figure 4 shows the LLE diagram for mixtures of [BMIM]-[SCN] with aromatic hydrocarbons, revealing the lower critical solution temperature (LCST). The minima of the binodal curves were at very low temperatures, and it was impossible to measure these points in acetone/dry ice bath using the static method. Generally, the trend observed on the solubility of [BMIM][SCN] in alkylbenzenes with respect to the alkyl chain length and benzene substitution is the same as was observed previously for many ILs. An increase in the alkyl chain of the substituent decreases the solubility of certain solvents in the IL.Comparing a few ionic liquids with different anions such as [BMIM]-
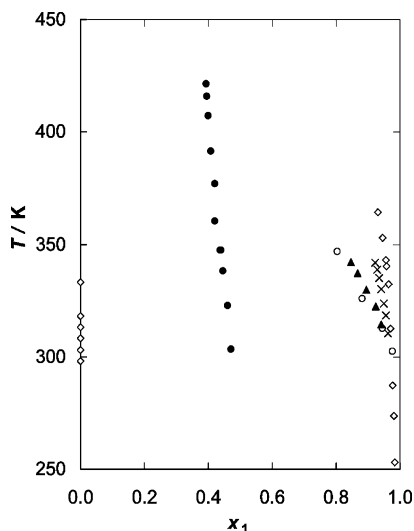
Phase Equilibria Study of the Binary Systems

J. Phys. Chem. B, Vol. 113, No. 18, 2009 **6401**

Figure 7. Experimental (liquid + liquid) phase equilibria of the {IL (1) + *n*-hexane (2)} binary systems; (◇) [BMIM][SCN]; (●) [BMIM]-[OcSO₄];[22] (○) [BMIM][CH₃SO₄];[23] (▲) [BMIM][PF₆];[25] (×) [BMIM]-[MDEGSO₄].[24]
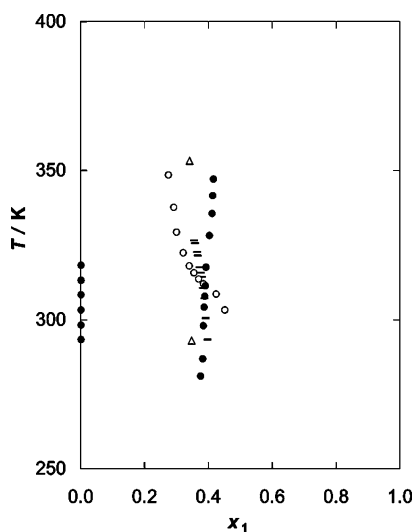

Figure 8. Experimental (liquid + liquid) phase equilibria of the {IL (1) + benzene (2)} binary systems; (●) [BMIM][SCN]; (○) [BMIM]-[CH₃SO₄];[23] (△) [BMIM][PF₆];[25] (-) [BMIM][MDEGSO₄].[24]

[CH₃SO₄], [BMIM][MDEGSO₄], and [BMIM][PF₆] with [BMIM]-[SCN], we can state that the solubility of benzene in the IL used in this work is similar (see Figure 8).[22–24] For this IL, the immiscibility gap in the liquid phase was (as for many ILs) from the low IL mole fraction (2×10^{-5}) to 0.4 (in benzene). The experimental data are listed in Table 3 in the SI. Aromatic hydrocarbons demonstrate that the interaction is most likely due to $\pi-\pi$ interactions between the benzene ring and the imidazolium-based IL. Only in the recently published data by Huo et.al.[25] were the solubilities of benzene and toluene in [BMIM][PF₆] lower at the same range of temperatures, but the method of measurement was different (with camera).

The experimental results for systems {[BMIM][SCN] + cycloalkanes} are given in Table 4S in the SI and in Figure 5. The (liquid + liquid) phase equilibria were observed for these systems as usual. The solubility of cycloalkanes in the [BMIM]-[SCN] decreases with an increase of the cycloalkane ring from C₆ to C₇; the solubility of cyclic molecules in the ILs is usually

better than those of long chain molecules, which was observed previously for many ILs.[10,12,22,24]

The solubility of [BMIM][SCN] in the THF also exhibits immiscibility in the liquid phase with a LCST, which is shown in Figure 6a, in comparison with other linear ethers, which are shown in Figure 6b. Experimental phase diagrams of LLE in the systems with ethers investigated in this work are characterized mainly by the following: (1) an increase in the alkyl chain length of the ether resulted in an increase in the upper critical solution temperature (UCST) (see Figure 6b); (2) the solubility is lower in dibutyl ether than in dipropyl ether, is lower in *n*-butyl-methyl ether than in MTBE, and is lower in ETBE than in MTBE; (3) the best solubility was observed in the THF and in the branched chain ether, MTBE; it has to be the result of the packing effect and the interstitial accommodation which is the better of the branched chain ethers (for the longer alkane chain, e.g., ethyl-, the solubility is worst); and (4) the inductive effect of the alkane chains of the branched chain ethers and butyl chain of the cation causes the stronger interaction of two dissimilar molecules.

The mutual (liquid + liquid) solubility of different solvents in the [BMIM][SCN] increases in the order alcohols > water > ethers > aromatic hydrocarbons > cycloalkanes > *n*-alkanes.

The effect of the anion on the solubility of discussed ILs in the tested solvents is the result of dissimilar molecules' hydrogen bonding and n–π or π–π interactions between the polar groups of ILs and the solvent. The stronger interaction on one side and the increased influence of the inductive effect of the longer alkyl chain of the solvent on the other side have a significant influence on the solubility.

Modeling

Correlation of (Solid + Liquid) Phase Equilibrium. Simple eq 1 relating the temperature, T^{SLE}, and the mole fraction of the IL, x_1, in respective solvent (only an alcohol and water) has been fitted to all of the sets of experimental SLE data[26]

$$-\ln x_2 = \frac{\Delta_{fus}H_2}{R}\left(\frac{1}{T^{SLE}} - \frac{1}{T_{fus,2}}\right) + \ln \gamma_2 \qquad (1)$$

where x_2, $\Delta_{fus}H_2$, T^{SLE}, $T_{fus,2}$, and γ_2 stand for the equilibrium mole fraction, enthalpy of fusion for the pure solvent, (solid + liquid) equilibrium temperature, melting temperature of the solvent, and the activity coefficient of the solvent in the saturated solution, respectively. The experimental data together with the calculated activity coefficients are listed in Table 1S in the SI (recalculated for the IL). The enthalpy of melting was assumed to be temperature-independent. Activity coefficient can be calculated from any equation expressing excess Gibbs energy (G^E) by using the Gibbs–Duhem equation. In this work, three equations were used to describe the experimental data, the UNIQUAC equation proposed by Abrams and Prausnitz,[27] the Wilson equation,[28] and the NRTL equation proposed by Renon and Prausnitz.[29] Molar volumes of solvents and the other physicochemical properties utilized in the equations are presented in Table 2. Parameters r_i and q_i (number of segments and external contacts of the molecule of type i, respectively) occurring in the UNIQUAC equation are related to the molar volumes by the following expressions

$$\begin{aligned} r_i &= 0.029281 V_{m,1} \\ Zq_i &= (Z-2)r_i + 2 \end{aligned} \qquad (2)$$

where Z denotes the coordination number (it was assumed that $Z = 10$) and where the bulk factor l_i was assumed to be equal

to 0 for the linear molecule. All of the applied equations have two adjustable parameters, P_1 and P_2 (for the NRTL equation, the α parameter is fixed, additionally), which are determined by minimization of the objective function $F(P_1,P_2)$, defined as follows

$$F(P_1, P_2) = \sum_{i=1}^{n} [T_{\exp,i} - T_{\text{calc},i}(x_i, P_1, P_2)]^2 \quad (3)$$

where n denotes the number of experimental points. In this work, the parameter α_{12}, a constant of proportionality similar to the nonrandomess constant of the NRTL equation ($\alpha_{12} = \alpha_{21} = 0.50$ or 0.55), was taken into account in the calculations. These values of parameter α_{12} in the SLE correlation have given the lowest root-mean-square deviations. The Marquardt algorithm for solving of the nonlinear least-squares problem was successfully used in this work. As a measure of the reliability of the correlations, the root-mean-square deviation of temperature, σ_T/K, has been calculated according to the following definition

$$\sigma_T = \left\{ \sum_{i=1}^{n} \frac{(T_{\exp,i} - T_{\text{calc},i})^2}{n - 2} \right\}^{1/2} \quad (4)$$

The values of the parameters and the corresponding root-mean-square deviations of temperature, σ_T/K, are presented in Table 3, and the resulting curves are summarizes together with the experimental points in Figures 1 and 2.

On the basis of obtained results, one can state that equations used are appropriate to provide a reliable description of SLE in the systems {[BMIM][SCN] (1) + alcohol or water (2)}. The average values of the root-mean-square deviations of temperature, σ_T/K, are 1.50, 0.80, and 0.62 K for the UNIQUAC, the Wilson, and the NRTL equations, respectively.

The mixtures investigated in this work show positive deviations from ideality in all of the different solvents. For each mixture, the experimental activity coefficients are listed in Table 1S in the SI. The differences from ideality were not significant in most of the systems. The values of the

TABLE 3: Results of Correlation of the Experimental (Solid + Liquid) Equilibrium Data of {[BMIM][SCN] (1) + Solvent (2)} Binary Systems by Means of the UNIQUAC, Wilson, and NRTL Equations along with Obtained Values of Parameters and Root-Mean-Square Deviations (RMSD) of Temperature (σ_T) as a Measure of Goodness of the Correlation

	parameters			rmsd		
	UNIQUAC	Wilson	NRTL	UNIQUAC	Wilson	NRTL
solvent	Δu_{12}	$\Delta \lambda_{12}$	Δg_{12}		(σ_T)/K	
	Δu_{21}/J·mol^{-1}	$\Delta \lambda_{21}$/J·mol^{-1}	Δg_{21}/J·mol^{-1}			
1-octanol	−409.70	7132.61	4479.69	0.99	0.49	0.16[a]
	1786.91	2029.16	6990.35			
1-nonanol	1386.51	2840.15	5006.09	2.12	1.21	0.62[b]
	−143.32	4679.45	5021.88			
1-decanol	1501.23	2773.60	5238.04	2.15	1.09	1.08[a]
	−211.60	5568.90	3527.95			
1-undecanol	810.00	4257.17	4699.81	1.39	0.77	0.61[a]
	341.55	4197.81	4696.02			
1-dodecanol	1560.02	3599.68	6484.57	2.03	0.59	0.70[a]
	−219.06	6552.06	4560.37			
water	1293.16	73792.47	−2739.35	0.30	0.65	0.54[b]
	2593.14	2265.46	7861.62			

[a] Calculated with nonrandomness parameter $\alpha = 0.50$. [b] Calculated with nonrandomness parameter $\alpha = 0.55$.

TABLE 4: Correlation of the (Liquid + Liquid) Equilibrium Data by Means of the NRTL Equation along with Parameters ($g_{12} - g_{22} = a_{12} + b_{12}T$) and ($g_{21} - g_{11} = a_{21} + b_{21}T$) and Deviations σ_x

	NRTL parameters							
	$(g_{12} - g_{22})$/(J·mol^{-1})			$(g_{21} - g_{11})$/(J·mol^{-1})			α	σ_x
	a_{12}	b_{12}	c_{12}	a_{21}	b_{21}	c_{21}		
n-hexane	−21312	170.96	−0.3294	10852	32.02	0.0717	0.1	0.0009
n-heptane	−16754	154.08	−0.3037	−2702	142.19	−0.1347	0.1	0.0010
n-octane	−27019	239.36	−0.4448	−2755	132.20	−0.0940	0.1	0.0005
n-nonane	36572	−137.25	0.1210	−3040	115.73	−0.0569	0.1	0.0008
n-decane	29610	−87.63	0.0537	−44201	315.98	−0.2992	0.1	0.0003
benzene	−2104	−8.79		−6963	88.95		0.2	0.0024
toluene	−1994	10.25		−5998	69.78		0.3	0.0003
ethylbenzene	−1437	3.881		−7209	84.68		0.2	0.0002
cyclohexane	15602	−51.42		−30.23	89.88		0.1	0.0018
cycloheptane	11475	−35.64		6014	71.18		0.1	0.0017
tetrahydrofuran	−5101	3.537		955.5	44.21		0.3	0.0016
di-*n*-propyl ether	12645	−43.29		12914	61.62		0.1	0.0014
di-*n*-butyl ether	7953	−22.16		13359	51.34		0.1	0.0010
di-*n*-pentyl ether	16497	−37.75		8524	60.06		0.1	0.0007
n-butylmethyl ether	8401	−34.67		17422	42.47		0.1	0.0024
tert-butylmethyl ether	6051	−33.15		5315	81.45		0.1	0.0007
tert-butylethyl ther	12221	−45.04		9770	66.27		0.1	0.0006

Phase Equilibria Study of the Binary Systems

J. Phys. Chem. B, Vol. 113, No. 18, 2009 **6403**

activity coefficients of the IL in the saturated solutions ranged from 1 to about 40.

Correlation of (Liquid + Liquid) Phase Equilibrium. In this study, one method was used to correlate the solute activity coefficients, γ_1, based on the NRTL model describing the excess Gibbs energy[29]

$$\frac{G^{\mathrm{E}}}{RT} = x_1 x_2 \left[\frac{\tau_{21} G_{21}}{x_1 + x_2 G_{21}} + \frac{\tau_{12} G_{12}}{G_{12} x_1 + x_2} \right] \qquad (5)$$

The description of this equation and the activity coefficient formula was presented by us earlier.[23]

The model adjustable parameters $(g_{12} - g_{22})$ and $(g_{21} - g_{11})$ were found by minimization of the objective function OF

$$\mathrm{OF} = \sum_{i=1}^{n} [(\Delta x_1)_i^2 + (\Delta x_1^*)_i^2] \qquad (6)$$

where n is the number of experimental points and Δx is defined as

$$\Delta x = x_{\mathrm{calc},i} - x_{\mathrm{exp},i} \qquad (7)$$

The root-mean-square deviation of the mole fraction was defined as follows

$$\sigma_{\mathrm{x}} = \left(\sum_{i=1}^{n} \frac{(\Delta x_1)_i^2}{n-2} + \sum_{i=1}^{n} \frac{(\Delta x_1^*)_i^2}{n-2} \right)^{1/2} \qquad (8)$$

In this work, the parameter α_{12}, a constant of proportionality similar to the nonrandomness constant of the NRTL equation ($\alpha_{12} = \alpha_{21} = 0.1, 0.2,$ or 0.3), was taken into account in the calculations. These values of parameter α_{12} in the LLE correlation have given the lowest root-mean-square deviations. The calculated values of the equation parameters and corresponding root-mean-square deviations are presented in Table 4. In binary systems, all deviations are in the range of σ_{x} from 0.0003 to 0.0024, being especially large for {[BMIM][SCN] + benzene or n-butylmethyl ether} systems.

For some mixtures under study of the (liquid + liquid) equilibrium data in the solvent-rich phase, it was impossible to detect phase changes by the visual method or by UV−vis spectra. It was assumed that the solubility in the dilute IL region was in the range of few experimental points measured in our experimental work with UV−vis spectra; this was found for n-hexane as shown in Table 2S in the SI, for the other n-alkanes, $x_1 \approx 2 \times 10^{-5}$, for benzene as shown in Table 3S in the SI, for toluene, $x_1 \approx 1.2 \times 10^{-3}$, for ethylbenzene, $x_1 \approx 6 \times 10^{-4}$, for cyclohexane as shown in Table 4S in the SI, for cycloheptane, $x_1 \approx 3 \times 10^{-5}$, for THF as shown in Table 5S in the SI, and for ethers, $x_1 \approx 1 \times 10^{-5}$. The results of the correlations are plotted in Figures 3−6. Positive deviations from ideality were found. The values of the activity coefficients of the IL in the saturated solution, calculated from the NRTL correlation, were higher than 1.

Conclusions

Phase equilibrium data, including SLE and LLE, for mixtures of 1-butyl-3-methylimidazolium thiocyanate [BMIM][SCN] ionic liquid and 1-alcohols, water, n-alkanes, benzene, alkylbenzenes, cycloalkanes, THF, or ethers have been measured. The results were compared to an analogous study of [BMIM]-[CH$_3$SO$_4$], [BMIM][OcSO$_4$], [BMIM][MDEGSO$_4$], and [BMIM]-[PF$_6$] in solvents similar to those used in this work. A comparison of phase diagrams indicates that an exchange of the anion, from thiocyanate to methylsulfate, octylsulfate,

2-(2-methoxyethoxy)-ethylsulfate, or hexafluorophosphate, changes the solubility of the IL mainly in n-alkanes. This is largely due to the specific interaction of the thiocyanate anion as other polar anions with polar or aromatic solvents. The SLE diagrams were observed versus LLE diagrams for [BMIM][SCN] with alcohols and water. The (solid + liquid) phase diagrams for the systems studied here were assumed as simple eutectic mixtures. Moreover, the solubility of the IL decreases as the length of the carbon chain of an alcohol or substituent on the benzene ring or the n-aliphatic chain in ethers increases.

The correlation of the SLE data was carried out by means of three commonly known G^{E} equations, UNIQUAC, Wilson, and NRTL. The NRTL equation was also used to correlate the LLE data with different interaction parameters and nonrandomness parameters. The results of the correlation of SLE and LLE were acceptable for all equations used, with an average rmsd of temperature of $\sigma_{\mathrm{T}} = 0.97$ K and $\sigma_{\mathrm{x}} = 0.0006$.

Supporting Information Available: Table 1S, experimental SLE data and the activity coefficients in the saturated solutions (alcohols, water); Tables 2S and 3S, experimental LLE data (aliphatic and aromatic hydrocarbons); Table 4S, experimental LLE data for cycloalkanes; Table 5S, experimental data for THF and ethers; GRS 1, DSC diagram of [BMIM][SCN]; GRS 2, TG/DSC diagram of [BMIM][SCN]; GRS 3−7, UV−vis spectra for {[[BMIM][SCN] + n-hexane, benzene, cyclohexane, or THF}. This material is available free of charge via the Internet at http://pubs.acs.org.

References and Notes

(1) Domańska, U.; Pobudkowska, A.; Królikowski, M. *Fluid Phase Equilib.* **2007**, *259*, 173–179.

(2) Holbrey, J. D.; López-Martin, I.; Rothenberg, G.; Seddon, K. S.; Silvero, G.; Zheng, X. *Green Chem.* **2008**, *10*, 87–92.

(3) Losada-Pérez, P.; Blesic, M.; Pérez-Sánchez, G.; Cerderiña, C. A.; Troncoso, J.; Romani, L.; Szydłowski, J.; Rebelo, L. P. N. *Fluid Phase Equilib.* **2007**, *258*, 7–15.

(4) Crosthwaite, J. M.; Aki, S. N. V.; Maginn, E. J.; Brennecke, J. F. *Fluid Phase Equilib.* **2005**, *228−228*, 303–309.

(5) Domańska, U. General Review of Ionic Liquids and their Properties. *Ionic Liquids in Chemical Analysis*; CRC Pres, Taylor & Francis Group: Abingdon, U.K., 2008; Chapter 1.

(6) Meindersma, G. W.; Podt, A.; de Hann, A. B. *J. Chem. Eng. Data* **2006**, *51*, 1814–1819.

(7) Mutelet, F.; Jaubert, J.-N. *J. Chromatogr. A* **2006**, *1102*, 256–267.

(8) Domańska, U.; Marciniak, A. *J. Phys. Chem. B* **2008**, *112*, 11100–11105.

(9) Domańska, U.; Marciniak, A. *J. Chem. Thermodyn.* **2008**, *40*, 860–866.

(10) Domańska, U.; Marciniak, A. *Fluid Phase Equilib.* **2007**, *260*, 9–18.

(11) Domańska, U.; Marciniak, M.; Królikowski, M. *J. Phys. Chem. B* **2008**, *112*, 1218–1225.

(12) Domańska, U.; Laskowska, M.; Marciniak, A. *J. Chem. Eng. Data* **2008**, *53*, 498–502.

(13) Domańska, U.; Żołek-Tryznowska, Z.; Królikowski, M. *J. Chem. Eng. Data* **2007**, *52*, 1872–1880.

(14) Domańska, U.; Paduszyński, K. *J. Phys. Chem. B* **2008**, *112*, 11054–11059.

(15) Domańska, U.; Laskowska, M. *J. Chem. Thermodyn.* **2009**, *41*, 645–650.

(16) Domańska, U.; Łachwa, J. *Fluid Phase Equilib.* **2002**, *198*, 1–14.

(17) Domańska, U.; Marciniak, M. *J. Chem. Eng. Data* **2005**, *50*, 2035–2044.

(18) Girard G. *Recommended Reference Materials for the Realization of Physicochemical Properties*; Marsh, K. N., Ed.; Blackwell Scientific Publications: Oxford, U.K., 1987; p 27.

(19) Domańska, U. *Fluid Phase Equilib.* **1986**, *26*, 201–220.

(20) Domańska, U.; Pobudkowska, A.; Eckert, F. *J. Chem. Thermodyn.* **2006**, *38*, 685–695.

(21) Domańska, U.; Pobudkowska, A.; Wiśniewska, A. *J. Solution Chem.* **2006**, *35*, 311–334.

(22) Domańska, U.; Pobudkowska, A.; Eckert, F. *Green Chem.* **2006**, *8*, 268–276.

(23) Domańska, U.; Marciniak, A. *Green Chem.* **2007**, *9*, 262–266.

(24) Domańska, U.; Marciniak, A. *J. Chem. Eng. Data* **2003**, *48*, 451–456.

(25) Huo, Y.; Xia, S.; Ma, P. *J. Chem. Eng. Data* **2008**, *53*, 2535–2539.

(26) Prausnitz, J. M.; Lichtenthaler, R. N.; Azevedo, E. G. *Molecular Thermodynamics of Fluid-Phase Equilibria*, 2nd ed.; Prentice-Hall Inc.: Engelwood Cliffs, NJ, 1986.

(27) Abrams, D. S.; Prausnitz, J. M. *AIChE J.* **1975**, *21*, 116–128.

(28) Wilson, G. M. *J. Am. Chem. Soc.* **1964**, *86*, 127–130.

(29) Renon, H.; Praustnitz, J. M. *AIChE J.* **1968**, *14*, 135–144.